World Conference on
Timber Engineering
Oslo 2023

DEVELOPING SLIMMER TIMBER WINDOW FRAME.

Katarzyna Ostapska[1], Tore Myrland Jensen[2], Lars Gullbreken[3], Petra Ruther[4],

ABSTRACT: Demand for the ever-increasing performance of windows when it comes to the thermal insulation properties requires, among other things, designing thinner timber frames. Structural strength and dimensional stability of wood under changing climate condition is of the key importance. In this paper the experimental and numerical investigation of the mechanical behaviour of the typical wooden window frame is presented. Based on the results, a new, slimmer timber window frame is designed and evaluated numerically. Large material savings and thermal insulation gains can be achieved with retaining required structural strength by use of optimized frames. The new frame design requires however proper design of hinge connection, protection against moisture accumulation and sufficient wood laminating for dimensional stability when exposed to varying climate conditions.

KEYWORDS: slim window timber frames, DIC, FEA, timber-to-steel screw connection

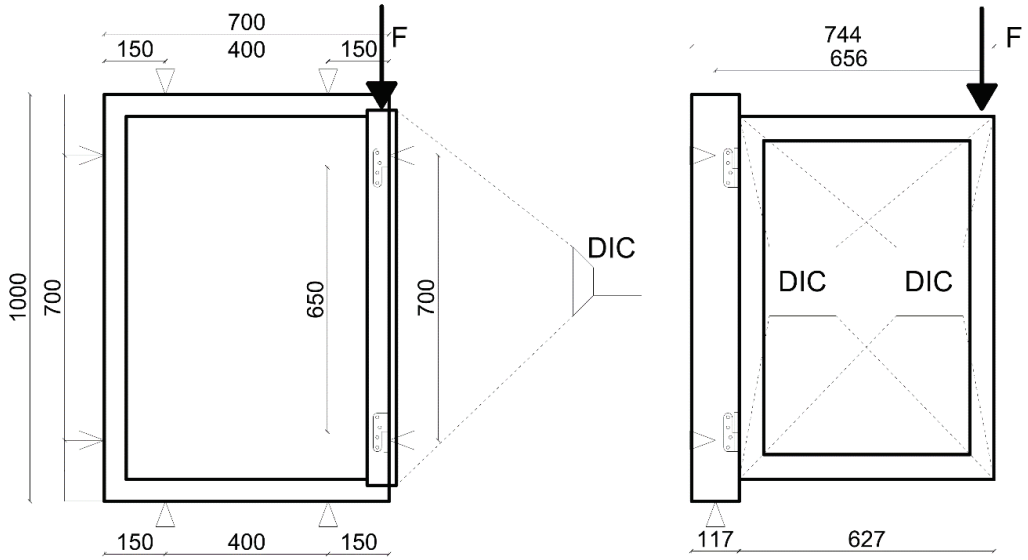

Figure 2.1: *Graphical scheme of the test set-up with optical measurement location.*

1 INTRODUCTION

Timber is the most popular material used for window framing. Its combination of high structural strength, good thermal isolation properties, and low carbon footprint makes it a natural choice for frame structures with crucial insulation functions. The further advantage of wood over plastic, aluminum and steel frames is its low energy demanding production and processing, renewability, and carbon storage qualities. To verify the design of the window, the thermal transmittance is commonly evaluated, e.g., with the formula shown in Equation (1) below:

$$U_w = \frac{U_{cg}A_g + \sum U_f A_f + \sum U_{eg}A_e}{A_t} \quad (1)$$

[1] Katarzyna Ostapska, SINTEF Community, Norway, Katarzyna.ostapska@sintef.no
[2] Tore Myrland Jensen, SINTEF Community, Norway, tor.m.jensen@sintef.no
[3] Lars Gullbreken, SINTEF Community, Norway, lars.gullbreken@sintef.no
[4] Petra Ruther, SINTEF Community, Norway, petra.ruther@sintef.no

https://doi.org/10.52202/069179-0497

where U- thermal transmittance, *A*- area measured in window plane, indexes: c-central, e-edge, f-frame, g-glass, t-total. The total thermal transmittance is thus dependent, among others, on the area of the frame in relation to the total area of the window in its plane. Reducing the area of the frame, not only decreases thermal transmittance but also increases glazing area that allows for energy gains due to irradiance [2], [3].

2 METHODS

2.1 EXPERIMENT DESIGN AND PROCEDURE

To establish current window frame capacity, the static loading test was performed on the 90-degree opened window frame with point force located at the top frame corner as shown in Figure 2.1. Such load case is important in case of exceptional load during fire emergency and evacuation. The estimated ultimate failure capacity based on the preliminary numerical simulation and analytical estimation was 1.5-2 kN and the load was applied discretely with 0.2 kN intervals by adding weight.

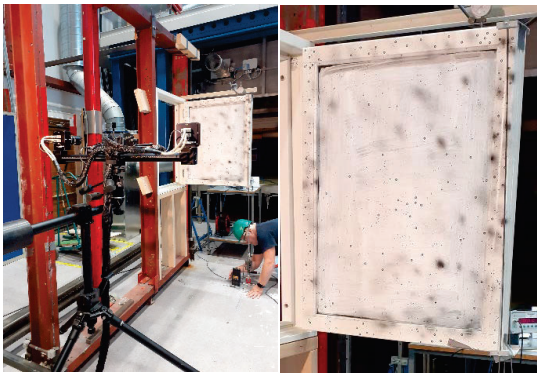

Figure 2.2: *Window frame and glazing painted for optical deformation tracking (left), image from the laboratory set-up.*

Deformations were measured optically on the whole window frame plane using commercial system of digital image correlation (DIC), ARAMIS, see Figure 2.2. Two cameras were used at a fixed distance and angle to produce the 3D displacement field that was required due to substantial out-of-plane deformation of the window during loading procedure.

2.2 NUMERICAL MODEL

The numerical mechanical model was built in the commercial software ABAQUS, where the internal stresses in wood were simulated with the use of finite element method (FEM) [1]. The geometry was based on the cross- section drawings of the original window design obtained from the producer (Røros Dører og Vinduer AS) and are shown together with subsequently modified frame sections in the Figure 2.3. The thinner frames dimensions are reduced across the thickness as the depth remains 117 mm. The thinnest frame design has wood volume reduced by 36%. This leads to the glass area increase by around 22% with the same external typical window dimensions of 1000x700mm.

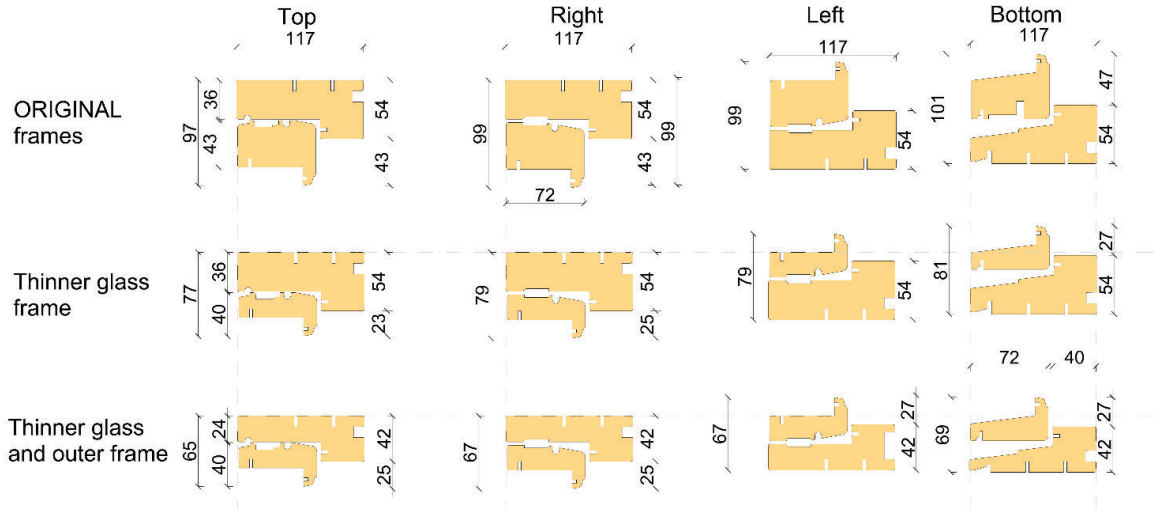

Figure 2.3. Cross section of the four frame parts for original (first row of drawings) and slim geometry after redesign (second and third raw).

Orthotropic elasticity was applied for wood material model, see Table 2.1, ideal elastic-plastic behaviour was assumed for steel hinged connection and elastic isotropic material model was used for glass (E = 50 GPa, ν=0.18).

Table 2.1*. Engineering constants for wood lamellas.*

Wood material properties [GPa]								
E_L	E_T	E_R	ν_{LR}	ν_{LT}	ν_{RT}	G_{LR}	G_{LT}	G_{RT}
10	0.6	0.6	0.5	0.5	0.8	0.6	0.6	0.06

The fixed steel-wood connection was used instead of screws for simplification in the preliminary model (model A). Screws were added to the model (model B) to

https://doi.org/10.52202/069179-0497

investigate the influence of their location and spacing on the force distribution in the hinge plate and timber. Screws were modelled with smooth shanks an assumed tied to the surrounding wood on the shank perimeter, see screw and hinge CAD geometry in Fig. 2.4.

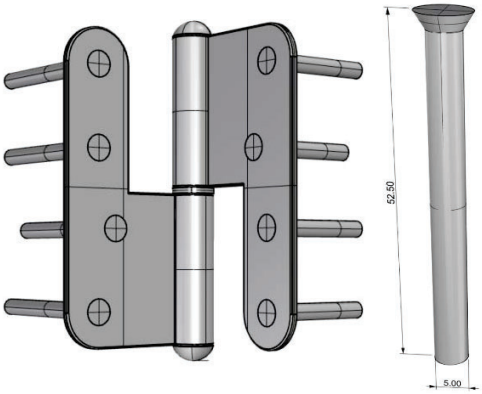

Figure 2.4: Hinge and screw model geometry.

Boundary conditions applied on the window encasing both in experiment and numerical analysis are depicted in Figure 2.5.

Finite element mesh was generated, see Figure 2.5 and 3.4, with continuous 3D solid elements. The two-layer glazing part was fixed to the timber frame part at the edges.

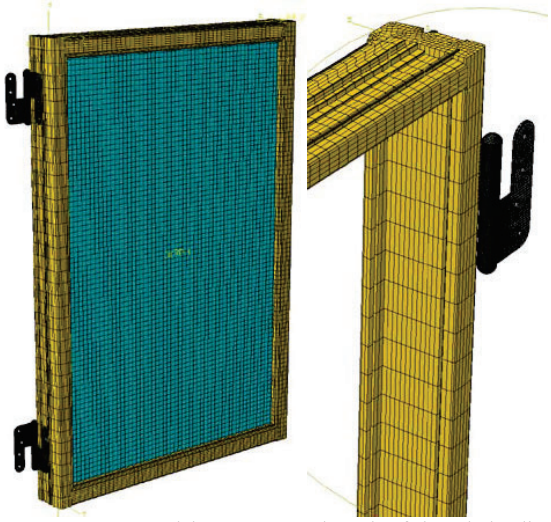

Figure 2.5: FE model geometry and mesh of the whole slim window with hinges (left) and timber frame corner detail (right).

3 RESULTS

3.1 DEFORMATIONS

The maximum measured total deformation corresponding to the maximum applied force of 1.6kN in the test was around 28 mm. The deformation is occurring in the hinge plates and the inner bolt undergoes localized bending and plastic hinge is formed.

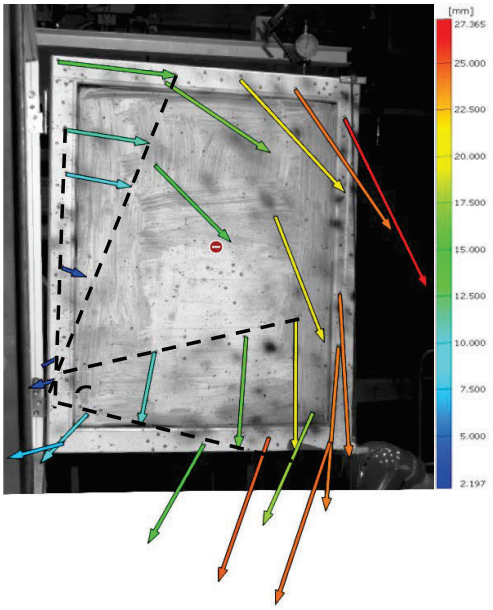

Figure 3.1: Deformations measured with DIC at 1.7kN load.

The window internal frame with glazing is rotating in plane initially as a whole, performing as a stiff shear plane component with slight in-plane shear deformations, see Figure 3.1. From the deformation field analysis, the centre of rotation is located in the vicinity of the bottom hinge. The frame is slender enough though and small out-of-plane force components caused by eccentricity of loading and boundary conditions (hinge fixings) lead to out-of-plane bending mode immediately. At this stage, large shear forces are transferred to the screw shank which leads to collapse of the frame element with glass.
Deformation modes obtained in the numerical analysis show similar behaviour and are depicted in the Figure 3.2.

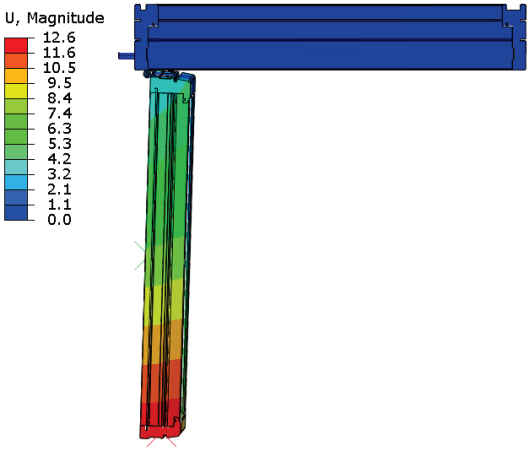

https://doi.org/10.52202/069179-0497

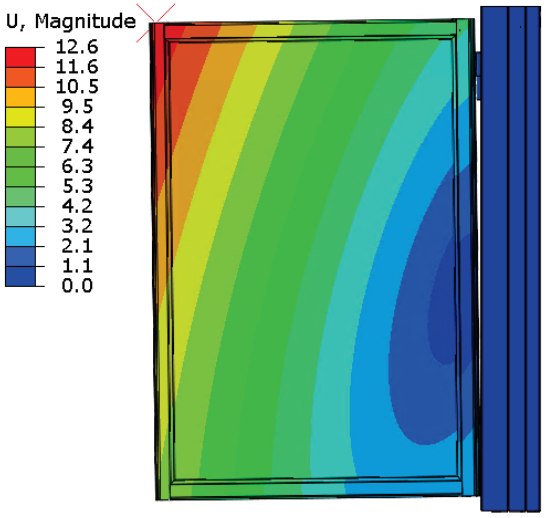

Figure 3.2: Deformation of the window in the numerical analysis from top and side view.

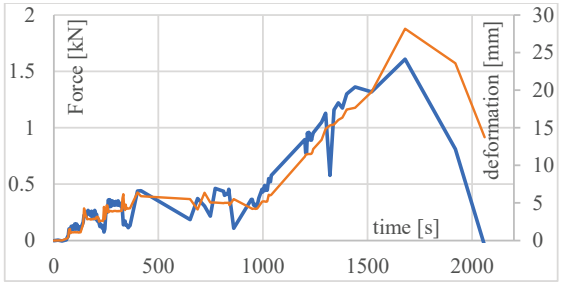

Figure 3.3: *Force (blue), load program (blue dashed) on the window frame and corresponding maximum deformation (red).*

3.2 STRESSES AND FAILURE MODE

3.2.1 STRESSES IN THE HINGE

Numerical simulation indicates the damage first occurs in the top plastic hinge, Figure 3.4, where the inner bolt starts to bend and steel plate bends because of resulting eccentricity. Based on that failure mechanism the window capacity was estimated at 1.5-2kN. Global stresses in timber frame sections are not exceeding the strength limits at the point of hinge connection failure.

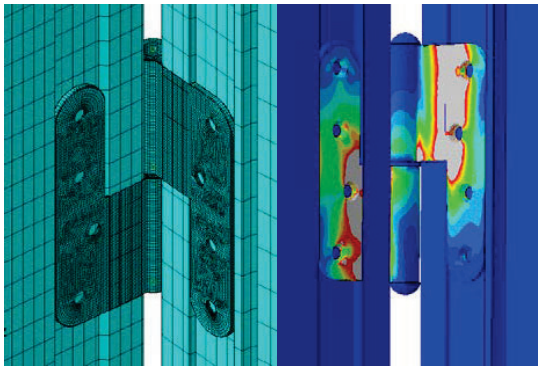

Figure 3.4: FE model of steel hinge connector (left) and stress distribution under 2kN Force (right). Gray colour areas indicate von Mises stress exceeding 250MPa.

3.2.2 STRESSES IN THE TIMBER FRAME

Timber frame is mostly not utilized in the performed test. Stresses in wood are exceeded only locally around the screw shanks, where critical concentrations start to occur as soon as 0.5kN load is reached.

Another stress concentration zone develops around the frame corners when the in-plane shear deformations and out-of-plane rotation starts. Rolling shear stresses and perpendicular to grain compression and tension in the corner of the bottom beam of the frame with glass are shown in figures 3.5 and 3.6. The presence of those stresses is a result of the twisting deformation in the glass-frame element occurring due to the eccentric and asymmetrical load.

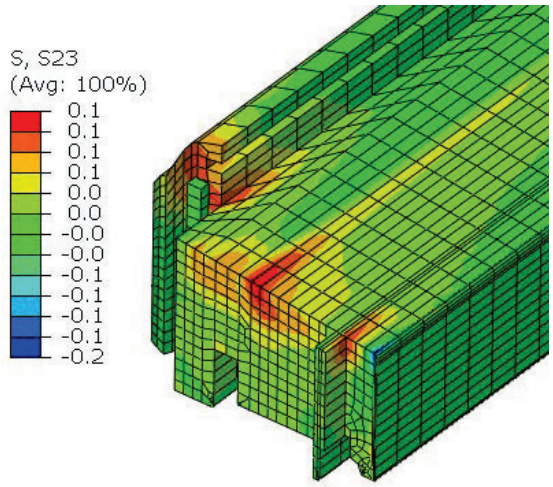

Figure 3.5: Rolling shear stresses in the end of the bottom beam of the window frame with glass at load of 1.6kN.

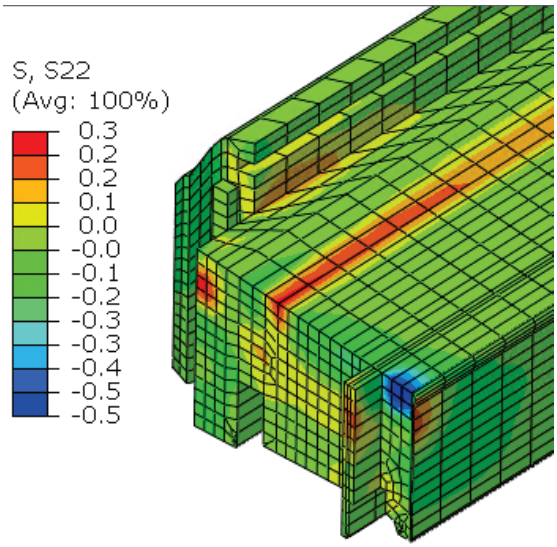

Figure 3.6: Perpendicular to grain stresses at the end of the bottom beam of the window glass frame at the load of 1.6kN.

https://doi.org/10.52202/069179-0497

3.2.3 STRESSES IN THE HINGE SCREWS AND IN WOOD AROUND THE SCREWS

Ultimate failure occurs in wood in shear around screws in the top hinge in the glass frame, see Figure 3.4.
The screws are not uniformly loaded since the plate of the connector is bended, and screw placement is not symmetrical. Forces in the screws from 1 to 4 were evaluated with the numerical model and their values are presented over the load history in Figures 3.8 and 3.9.
Screws are loaded both axially as intended and bended and pressed into the wood perpendicularly to the grain. This transverse force distribution is shown in the Figure 3.8. The top screw is subjected to the half of the total transverse force transferred from the glass frame through the hinge. The bottom screw shares only 8% of the transverse load. Axial forces in the screws are shown in the Figure 3.9. Screw number 3, the second from the top, is subject to the axial withdrawal, while remaining screws no 1, 2, and 4 (see Figure 3.7 left) are axially pressed into the timber.

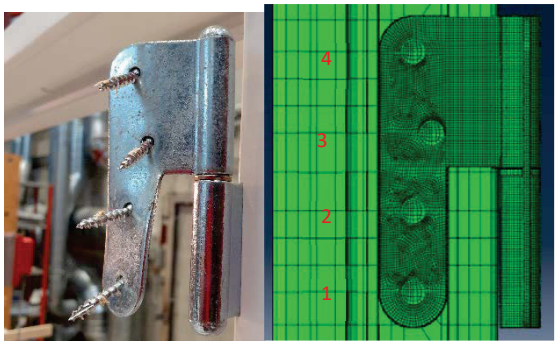

Figure 3.7: Screws in hinge after failure (left) and the numerical model with mesh and screw numbers (right).
The negative force (compression) transferred via screws 4,2, and 1 is in equilibrium with the positive (tension) force transferred by screw no 3. The screws do not cooperate in axial resistance to withdrawal, but are counteracting the hinge plate bending.

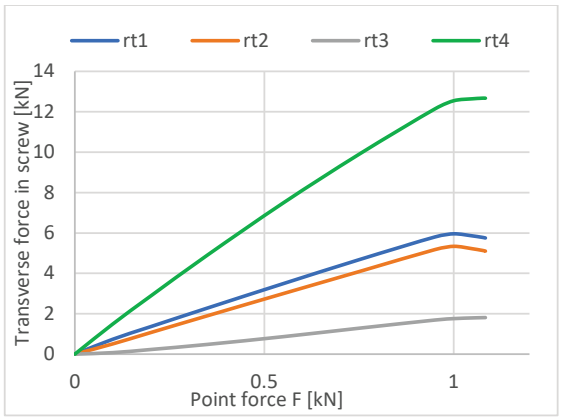

Figure 3.8: Distribution of transverse forces in the screws through loading history.

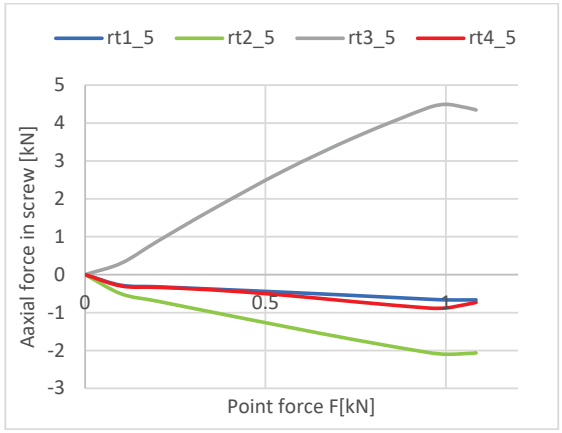

Figure 3.9: Deformation of the window in the numerical analysis from top and side view.

3.3 EXPERIMENTAL AND NUMERICAL RESULTS: COMPARISON

Window frame test shows plastic deformation in the top hinge and ultimate failure of wood around the screws in combined shear and perpendicular to grain tension at ca 1.6kN force, see Figure 3.7 to the left. The block shear failure in screws leads to sudden glass-frame collapse. The ductile deformation and onset of damage in wood-screw area can be visible much earlier, at around 0.6kN force (see both numerical and experimental force-displacement curves in Figure 3.10) and at around 1kN for the thinner frame according to the simulation.
The numerical analysis leads to good prediction of initial damage mechanism that can be set as the capacity limit for window frame in the considered load scenario.
The difference in the apparent stiffness can be mainly subjected to the different eccentricity of the initial set-up and force position in relation to the gravity centre of the glass-frame. The apparent stiffness is considerably higher for the thin frame that has 4 layer glass pack compared to the original 3-layer glass pack in the thick frame or the 3-layer glass pack thin frame model.

https://doi.org/10.52202/069179-0497

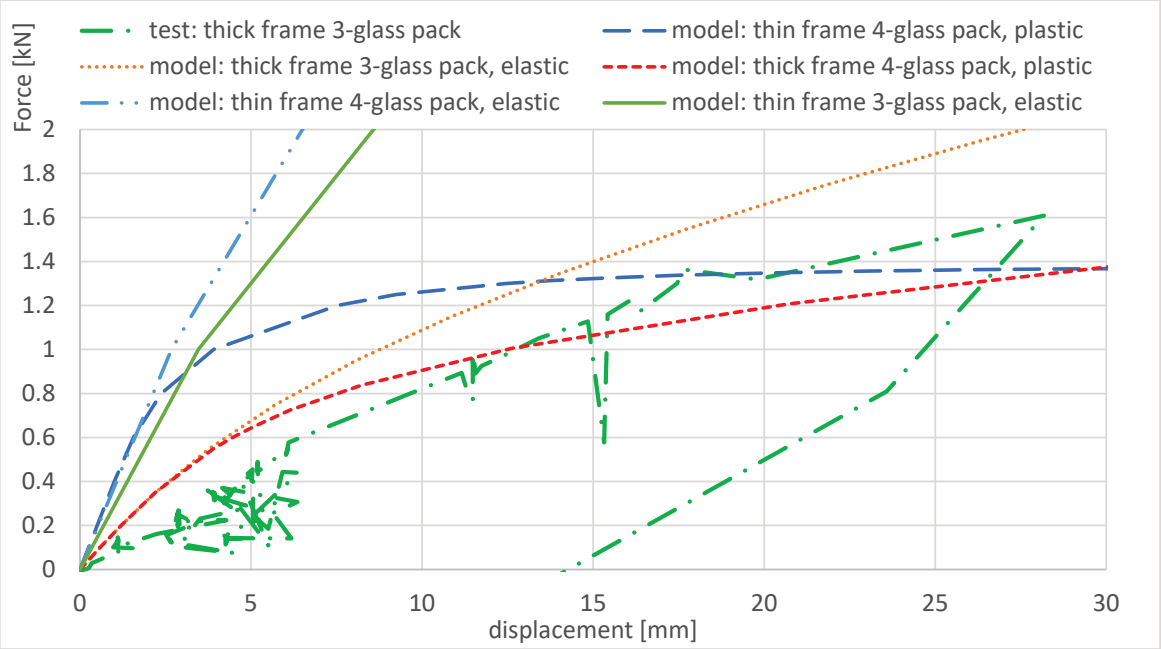

Figure 3.10: Force- displacement curves from the test and from the numerical model simulations for different settings.

4 DISCUSSION

Based on the validation via experiments, the numerical model of the thick frame with 3-layer glass pack was further developed into variants with the slim frame design and 3 and 4-glass packs. The new, slimmer design of the frame is subject to more impact from the localized failure around the screws due to the decreased dimensions so the detail study of the screw around the stresses was performed. The simulation shows that force distribution in screws is not as intended in the considered design case and leads to only one screw being effectively transferring withdrawal loads. The new shape of the hinge plate and optimized placement of the screws could improve the design. The analysis focuses on static strength and does not consider moisture variation that can introduce stresses and dimensional changes. Those dimensional changes due to moisture fluctuations would further increase the stresses localized in the frame corners that are more vulnerable due to the decreased area of the gluing.

During the development of the slimmer frame design, the need for rethinking the connection arose. The localized screwed in connection causes damage in slim frame to occur in wood shear failure (at 1-1.2kN according to the simulation) before hinge plasticisation. Better distribution of the stresses via use of linear hinge or a clamp should be considered in future investigations.

5 CONCLUSIONS

Current wood window frame thickness can be decreased from the structural point of view to improve thermal properties, increase glazing area, and save raw wood material and costs. The dimensional stability of the window over cycling moisture load is more critical than the static strength. The glass pack is found to be the main stiffness source for the frame. Screw configuration in the commonly used hinge is not transferring forces optimally and uniformly and can be optimized or redesigned.

ACKNOWLEDGEMENT

Authors acknowledge the Norwegian Research Council funding the HVIT project (Highly Insulating Windows and Doors with integrated Technology) and the project partner *Røros Vinduer og Dører AS* company.

REFERENCES

[1] Bathe K.-J.: Finite-Elemente-Methoden. Springer-Verlag Berlin Heidelberg New York, 2002.

[2] A. Gustavsen, B. P. Jelle, D. Arasteh, C. Kohler, State-of-the-Art Highly Insulating Window Frames – Research and Market Review, Project report, *SINTEF Building and Infrastructure* 2007.

[3] N. Van Den Bossche, L. Buffel, A. Janssens, Thermal Optimization of Window Frames. In: *Energy Procedia*, 78, pages 2500-2505, 2015.